

END-TO-END LABEL UNCERTAINTY MODELING FOR SPEECH EMOTION RECOGNITION USING BAYESIAN NEURAL NETWORKS

Navin Raj Prabhu^{*†} Guillaume Carbajal^{*} Nale Lehmann-Willenbrock[†] Timo Gerkmann^{*}

^{*}Signal Processing, Universität Hamburg, Germany

[†]Industrial and Organizational Psychology, Universität Hamburg, Germany

{navin.raj.prabhu, guillaume.carbajal, nale.lehmann-willenbrock, timo.gerkmann}@uni-hamburg.de

ABSTRACT

Emotions are subjective constructs. Recent end-to-end speech emotion recognition systems are typically agnostic to the subjective nature of emotions, despite their state-of-the-art performances. In this work, we introduce an end-to-end Bayesian neural network architecture to capture the inherent subjectivity in emotions. To the best of our knowledge, this work is the first to use Bayesian neural networks for speech emotion recognition. At training, the network learns a distribution of weights to capture the inherent uncertainty related to subjective emotion annotations. For this, we introduce a loss term which enables the model to be explicitly trained on a distribution of emotion annotations, rather than training them exclusively on mean or gold-standard labels. We evaluate the proposed approach on the AVEC'16 emotion recognition dataset. Qualitative and quantitative analysis of the results reveal that the proposed model can aptly capture the distribution of subjective emotion annotations with a compromise between mean and standard deviation estimations.

Index Terms— Bayesian neural networks, end-to-end speech emotion recognition, uncertainty, subjectivity, label distribution learning

1. INTRODUCTION

While individual subjective emotional experiences may be accessed using self-report surveys [1], expressions of emotions are embedded in social context, which makes them inherently dynamic and subjective interpersonal phenomena [2, 3]. One way in which emotions become expressed in social interactions and therefore accessible for social signal processing concerns speech signals. Speech emotion recognition (SER) research spans roughly two decades [4], with ever improving state-of-the-art results. As a consequence, affective sciences and SER research has shown increasing prominence in high-critical and socially relevant domains, e.g. health, security and employee well-being [4, 5].

Common SER approaches rely on hand-crafted features to predict mean [6] or gold-standard [7] emotion labels. Recently, end-to-end deep neural networks (DNNs) have been shown to deliver state-of-the-art arousal and valence predictions [8, 9], by *learning* features rather than relying on hand-crafted features. Despite their state-of-the-art results, they are often agnostic to the subjective nature of emotions and the resulting label uncertainty [10, 11], thereby inducing limited reliability in SER [4]. However, for any real-world application context, it is crucial that SER systems should not only

deliver gold-standard predictions but also account for subjectivity based confidence measures [12, 4].

Han et al., [10, 7] pioneered uncertainty modeling in SER using a multi-task framework to also predict the standard deviation of emotion annotations. However, their work relied on hand-crafted features and a multi-task criterion which does not model any distribution. Sridhar et al., [11] introduced a dropout-based model to estimate uncertainties. However, their model still relied on hand-crafted features and was not explicitly trained on annotation distributions.

Uncertainty in machine learning has been categorized into two types. *Aleatoric* uncertainty captures data inherent noise (label uncertainty) whereas *epistemic* uncertainty accounts for the model parameters and structure (model uncertainty) [13]. Stochastic and probabilistic models have mainly been deployed for uncertainty modeling, using auto-encoder architectures [14], neural processes [15], and Bayesian neural networks (BNN) [16]. Bayes by Back-propagation (BBB) for BNNs, formulated by Blundell et al., [16], uses simple gradient updates to optimize weight distributions. This approach can be easily extended to end-to-end models, which makes it a promising candidate for end-to-end uncertainty SER.

In this paper, we propose to use an end-to-end BBB-based BNN architecture for SER. To the best of our knowledge, this is the first time a BNN is used for SER. In contrast to [7, 11], the model can be explicitly trained on a distribution of emotion annotations. For this, we introduce a loss term that promotes capturing *aleatoric* uncertainty (label uncertainty) rather than exclusively capturing *epistemic* uncertainty (model uncertainty). Finally, we show that our proposed model trained on the loss term can aptly capture label uncertainty.

The rest of the paper is organized as follows. In Section 2, we present related background. In Section 3, we introduce the proposed end-to-end BNN SER model. In Section 4, we explain the experimental setup. In Section 5, we present the results and raise discussions on them.

2. BACKGROUND

2.1. Ground-truth labels

As opposed to emotions as inner subjective experiences [1], we focus on emotional expressions as visible behaviors that others subjectively perceive and can respond to. A common framework for analyzing the expression of emotion in social interactions is pleasure-arousal theory [17, 18], which describes emotional experiences in two continuous, bipolar, and orthogonal dimensions: pleasure-displeasure (*valence*) and activation-deactivation (*arousal*). A crucial challenge in studying emotional expressions within the arousal and valence framework concerns the significant degree of

This work was supported by the Landesforschungsförderung Hamburg (LFF-FV79), under the "Mechanisms of Change in Dynamic Social Interaction" project.

subjectivity surrounding them [4, 10, 19]. To tackle this, annotations $\{y_1, y_2, \dots, y_a\}$ for emotions are collected from a annotators [20, 21]. The *ground-truth label* is then obtained as the mean m over all annotations from a annotators [6, 22],

$$m = \frac{1}{a} \sum_{i=1}^a y_i. \quad (1)$$

Alternatively, an evaluator-weighted mean has been proposed and referred to as the *gold-standard* \hat{m} [23, 8, 9]. In this paper, however, we do not utilise the gold-standard and stick to the mean m .

2.2. Point estimates in SER

Given a raw audio sequence of T frames $\mathcal{X} = [x_1, x_2, \dots, x_T]$, typically, the goal is to estimate the ground-truth label m_t for each time frame $t \in [1, T]$, referred to as \hat{m}_t . The concordance correlation coefficient (CCC), which takes both linear correlations and biases into consideration, has been widely used as a loss function for this task. For Pearson correlation r , the CCC between the ground-truth label m and its estimate \hat{m} , for T frames, is formulated as

$$\mathcal{L}_{\text{CCC}}(m) = \frac{2r\sigma_m\sigma_{\hat{m}}}{\sigma_m^2 + \sigma_{\hat{m}}^2 + (\mu_m - \mu_{\hat{m}})^2}, \quad (2)$$

where $\mu_m = \frac{1}{T} \sum_{t=1}^T m_t$, $\sigma_m^2 = \frac{1}{T} \sum_{t=1}^T (m_t - \mu_m)^2$, and $\mu_{\hat{m}}$, $\sigma_{\hat{m}}^2$ are obtained similarly for \hat{m} .

Early approaches relied on hand-crafted features as inputs to estimate CCC. End-to-end DNNs which circumvent the limitations of hand-crafted and -chosen features have been deployed to yield state-of-the-art performance [24, 8, 9]. Notwithstanding their performance, end-to-end DNNs are trained exclusively on ground truth labels and therefore cannot account for annotator subjectivity.

2.3. Uncertainty modeling in SER

Han et al. quantified label uncertainty using a statistical estimate, the perception uncertainty s defined as the unbiased standard deviation of a annotators [10, 7]:

$$s = \sqrt{\frac{1}{a-1} \sum_{i=1}^a (y_i - m)^2}. \quad (3)$$

They proposed a multi-task framework to additionally estimate s along with m . However, the model only accounts for the standard deviation of a annotations, rather than the whole distribution in itself. Thereby, they are susceptible to unreliable s estimates for lower values of a and sparsely distributed annotations.

Sridhar et al. introduced a Monte-Carlo dropout-based uncertainty model, to obtain stochastic predictions and uncertainty estimates [11]. The model is trained exclusively on ground-truth labels m rather than the distribution of annotations, thereby only capturing the model uncertainty and not the label uncertainties.

3. END-TO-END LABEL UNCERTAINTY MODEL

In order to better represent subjectivity in emotional expressions, we propose to estimate the *emotion annotation distribution* \mathcal{Y}_t for each frame t . While the true distributional family of \mathcal{Y}_t is unknown, we assume, for simplicity, that it follows a Gaussian distribution:

$$\mathcal{Y}_t \sim \mathcal{N}(m_t, s_t). \quad (4)$$

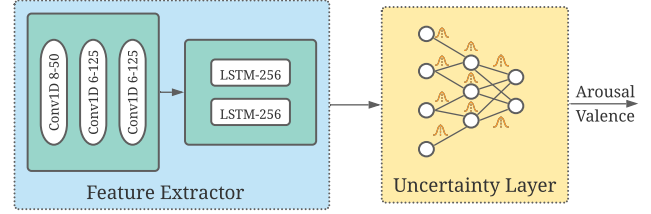


Fig. 1: Overview of the proposed architecture. Blue denotes layers with deterministic weights and yellow with probabilistic weights.

Thus, the goal is to obtain an estimate $\hat{\mathcal{Y}}_t$ of \mathcal{Y}_t and infer both m_t and s_t from realizations of $\hat{\mathcal{Y}}_t$.

3.1. End-to-end DNN architecture

We propose an end-to-end architecture which uses a feature extractor to learn temporal-paralinguistic features from x_t , and an uncertainty layer to estimate \mathcal{Y}_t (see Fig. 1). The feature extractor, inspired from [8], consists of three Conv1D layers followed by two stacked long-short term memory (LSTM) layers. The uncertainty layer is devised using the BBB technique [16], comprising three BBB-based MLP.

3.2. Model uncertainty loss

Unlike a standard neuron which optimizes a deterministic weight w , the BBB-based neuron learns a probability distribution on the weight w by calculating the variational posterior $P(w|\mathcal{D})$ given the training data \mathcal{D} [16]. Intuitively, this regularizes w to also capture the inherent uncertainty in \mathcal{D} .

Following [16], we parametrize $P(w|\mathcal{D})$ using a Gaussian distribution $\mathcal{N}(\mu_w, \sigma_w)$. For non-negative σ_w , we re-parametrize the standard deviation $\sigma_w = \log(1 + \exp(\rho_w))$. Then, $\theta = (\mu_w, \rho_w)$ can be optimized using simple backpropagation, making the optimization in BBB very much similar to that of a standard neuron.

For an optimized θ , the predictive distribution $\hat{\mathcal{Y}}_t$ for an audio frame x_t , is given by $P(\hat{\mathcal{Y}}_t|x_t) = \mathbb{E}_{P(w|\mathcal{D})}[P(\hat{\mathcal{Y}}_t|x_t, w)]$, where $\hat{\mathcal{Y}}_t$ are realizations of $\hat{\mathcal{Y}}_t$. Unfortunately, the expectation under the posterior of weights is intractable. To tackle this, the authors in [16] proposed to learn θ of a weight distribution $q(w|\theta)$, the variational posterior, that minimizes the Kullback-Leibler (KL) divergence with the true Bayesian posterior, resulting in the negative evidence lower bound (ELBO),

$$f(w, \theta)_{\text{BBB}} = \text{KL}[q(w|\theta)||P(w)] - \mathbb{E}_{q(w|\theta)}[\log P(\mathcal{D}|w)]. \quad (5)$$

Stochastic outputs in BBB are achieved using multiple forward passes n with stochastically sampled weights w , thereby modeling $\hat{\mathcal{Y}}_t$ using the n stochastic estimates. To account for the stochastic outputs, (5) is approximated as,

$$\mathcal{L}_{\text{BBB}} \approx \sum_{i=1}^n \log q(w^{(i)}|\theta) - \log P(w^{(i)}) - \log P(\mathcal{D}|w^{(i)}). \quad (6)$$

where $w^{(i)}$ denotes the i^{th} weight sample drawn from $q(w|\theta)$. The BBB window-size b controls how often new weights are sampled for time-continuous SER. The degree of uncertainty is assumed to be constant within this time period.

3.3. Label uncertainty loss

Inspired by [13], we introduce a KL divergence-based loss term as a measurement of distribution similarity to explicitly fit our model to the label distribution \mathcal{Y}_t :

$$\mathcal{L}_{\text{KL}} = f(\mathcal{Y}_t \| \hat{\mathcal{Y}}_t)_{\text{KL}} = \int \mathcal{Y}_t(x) \log \frac{\mathcal{Y}_t(x)}{\hat{\mathcal{Y}}_t(x)} dx. \quad (7)$$

The KL divergence is asymmetric, making the order of distributions crucial. In this work, the true distribution \mathcal{Y}_t is followed by its estimate $\hat{\mathcal{Y}}_t$, promoting a mean-seeking approximation rather than a mode-seeking one and capturing the full distribution [25].

3.4. End-to-end uncertainty loss

The proposed end-to-end uncertainty loss is formulated as,

$$\mathcal{L} = \mathcal{L}_{\text{CCC}}(m) + \mathcal{L}_{\text{BBB}} + \alpha \mathcal{L}_{\text{KL}}. \quad (8)$$

Intuitively, $\mathcal{L}_{\text{CCC}}(m)$ optimizes for mean predictions m , \mathcal{L}_{BBB} optimizes for BBB weight distributions, and \mathcal{L}_{KL} optimizes for the label distribution \mathcal{Y}_t . For $\alpha = 0$, the model only captures model uncertainty (MU). For $\alpha = 1$, the model also captures *label uncertainty* ($+LU$). $\mathcal{L}_{\text{CCC}}(m)$ is used as part of \mathcal{L} to achieve faster convergence and jointly optimize for mean predictions. Including $\mathcal{L}_{\text{CCC}}(m)$ might lead to better optimization of the feature extractor [8, 26]. Moreover, it may also contribute towards modeling label distribution.

4. EXPERIMENTAL SETUP

4.1. Dataset

To validate our model, we use the AVEC'16 challenge's [22] subset of the RECOLA dataset [20]. Multimodal signals were recorded from 27 subjects, and in this work we only utilize the audio signals collected at 16 kHz. The dataset consists of continuous arousal and valence annotations by $a = 6$ annotators at 40 ms frame-rate, and post-processed with local normalization and mean filtering. The arousal and valence annotations are distributed on average with $\mu_m = 0.01$ and $\mu_s = 0.11$, and $\mu_s = 0.23$ and $\mu_s = 0.14$ respectively, where $\mu_s = \frac{1}{T} \sum_{t=1}^T s_t$. The dataset is divided into speaker disjoint partitions for training, development and testing, with nine 300 s recordings each. As the annotations for the test partition in the dataset are not publicly available, all results are computed on the development partition.

4.2. Baselines

To validate the mean estimates m of our model, we use the AVEC'16 baseline [22] and Han et al. [7]. For the end-to-end baseline (E2E baseline), we use the proposed architecture but with the uncertainty layer replaced by a vanilla MLP. The resulting end-to-end baseline has 1,446,634 trainable parameters, in contrast to the 1,643,110 parameters in the models comprising the uncertainty layer.

4.3. Choice of hyperparameters

The hyperparameters of the *feature extractor* (e.g. kernel sizes, filters, stride) are adopted from [26]. A similar extractor with the same hyperparameters has been used in several multimodal emotion recognition tasks with state-of-the-art performance [9, 26].

As the *prior distribution* $P(w)$, [16] recommend a mixture of two Gaussians, with zero means and standard deviations as $\sigma_1 >$

	Arousal		Valence	
	$\mathcal{L}_{\text{CCC}}(m)$	$\mathcal{L}_{\text{CCC}}(s)$	$\mathcal{L}_{\text{CCC}}(m)$	$\mathcal{L}_{\text{CCC}}(s)$
AVEC'16 [22]	0.796	-	0.455	-
Han et al. [7]	0.779	-	0.534	-
E2E baseline	0.773	-	0.323	-
Model uncertainty	0.736	0.076	0.270	0.036
+ Label uncertainty	0.710	0.340	0.253	0.042

Table 1: Performance comparison on mean m and standard deviation s estimates. Larger CCC indicate improved performance.

	Arousal	Valence
Model uncertainty	0.690	0.633
+ Label uncertainty	0.258	0.405

Table 2: Performance comparison on label distribution estimation \mathcal{Y} , in terms of \mathcal{L}_{KL} . Lower KL indicates improved performance.

σ_2 and $\sigma_2 \ll 1$, thereby obtaining a spike-and-slab prior with a heavy tail and concentration around zero mean. But in our case, we do not need mean centered predictions as \mathcal{Y} does not follow such a distribution, as seen in Section 4.1. In this light, following the standard approach of BBB for BNNs, we propose to use a simple Gaussian prior with unit standard deviation $\mathcal{N}(0, 1)$.

The μ_w and ρ_w of the *posterior distribution* $P(w|D)$ are initialized uniformly in the range $[-0.1, 0.1]$ and $[-3, -2]$ respectively. The ranges were fine-tuned using grid search for maximized \mathcal{L}_{KL} at initialization on the train partition.

It is computationally expensive to sample new weights at every time-step (40 ms) and also the level of uncertainties varies rather slowly. In this light, we set *BBB window-size* $b = 2$ s (50 frames). The same window-size is also used for median filtering, the sole post-processing technique used. The *number of forward passes* in (6) is fixed to $n = 30$, with the time-complexity in consideration.

For training, we use the Adam optimizer with a learning rate of 10^{-4} . The batch size used was 5, with a sequence length of 300 frames, 40 ms each and 12 s in total. Dropout with probability 0.5 was used in the feature extractor to prevent overfitting. All the models were trained for a fixed 60 epochs. The best model is selected and used for testing when best \mathcal{L} is observed on train partition.

4.4. Validation metrics

To validate our mean estimates, we use $\mathcal{L}_{\text{CCC}}(m)$, a widely used metric in literature [8, 26, 7]. To validate the label uncertainty estimates, we use $\mathcal{L}_{\text{CCC}}(s)$, along with \mathcal{L}_{KL} . $\mathcal{L}_{\text{CCC}}(s)$, previously used in [10], only validates the performance on s , and ignores performances on m . In this light, we additionally use \mathcal{L}_{KL} which takes a holistic approach by validating both m and s performances. However, the metric makes a Gaussian assumption on \mathcal{Y}_t and hence can be biased. Thus, we use both these metrics for the validation with their respective benefits under consideration.

5. RESULTS AND DISCUSSION

5.1. Mean and standard deviation estimation

Table 1 shows the average performance in terms of CCC for the mean m and standard deviation s estimations, $\mathcal{L}_{\text{CCC}}(m)$ and $\mathcal{L}_{\text{CCC}}(s)$ respectively. Comparisons with respect to s are not presented for the three baselines as these approaches do not estimate s .

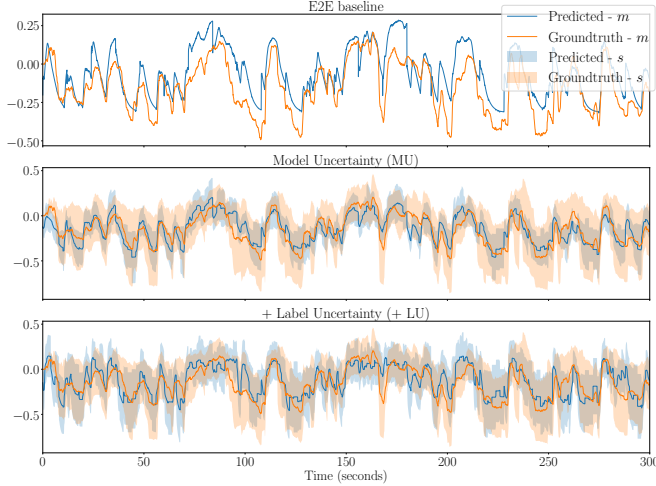


Fig. 2: Results obtained for a test subject for arousal.

We see that the E2E baseline is outperformed by Han et al. [7] and AVEC’16 [22] for both arousal and valence, in terms of $\mathcal{L}_{CCC}(m)$. This might come from the reason that the complete RECOLA dataset was used for training in [8], from whom our end-to-end feature extractor was inspired from. In contrast, we trained our model on a subset of the dataset [22] as we did not have access to the complete RECOLA dataset [20]. At the same time, end-to-end models are generally inefficient on small datasets compared to “handcrafted” models as they would require large amount of data to learn features.

Secondly, we see that our uncertainty models, MU and + LU, are outperformed by the baselines in terms of $\mathcal{L}_{CCC}(m)$. A potential reason for this could be the complexity of the end-to-end loss \mathcal{L} which introduces a trade-off between the mean predictions m , the distribution estimation \mathcal{Y} , and the weight optimization $P(w|D)$. Moreover, unlike the baselines which are solely optimized for m estimations, our uncertainty models additionally infer s from stochastic outputs with a more complex and crucial goal of capturing the label distribution \mathcal{Y} . By capturing \mathcal{Y} , the proposed models account for subjectivity in emotion and promote reliability in SER systems.

Finally, we see that + LU outperforms MU in terms of $\mathcal{L}_{CCC}(s)$, but makes a compromise on $\mathcal{L}_{CCC}(m)$. For example, in arousal, + LU improves in terms of $\mathcal{L}_{CCC}(s)$ from 0.076 to 0.340, while compromising on $\mathcal{L}_{CCC}(m)$ from 0.736 to 0.710. This reveals, that by also optimizing \mathcal{L}_{KL} , our model can better account for subjectivity in emotions, but further introduces a tradeoff between mean and label distribution estimations.

5.2. Distribution estimation

Table 2 shows the performance of our uncertainty models in terms of \mathcal{L}_{KL} . As expected, we see that \mathcal{L}_{KL} decreases when using label uncertainty since + LU also optimizes \mathcal{L}_{KL} . To further validate the results, we plot the distribution estimations for a test subject for arousal and valence, seen in Figures 2 and 3 respectively. From the figures, backing the results in Table 2, one may see that + LU best captures the subjectivity in emotions, while MU is optimized more for predictions centered on the mean and strict standard deviations.

Secondly, we see that the + LU model can fit quite accurately the ground truth distribution \mathcal{Y}_t on the arousal dimension. However, performs poorly on the valence dimension. Note that it is commonly observed in SER literature that the audio modality insufficiently ex-

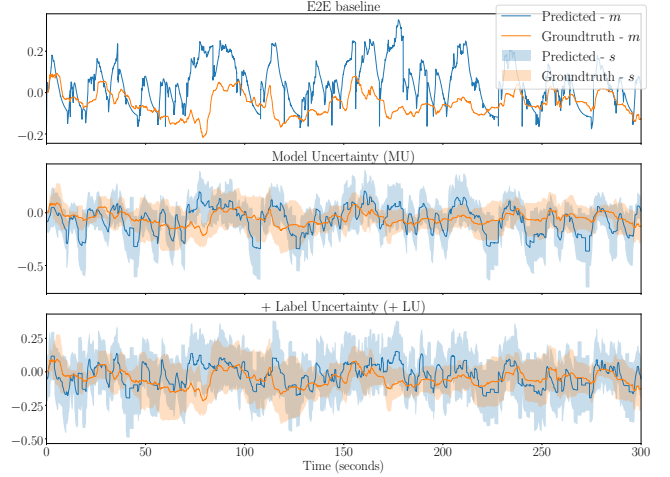


Fig. 3: Results obtained for a test subject for valence.

plains valence [8, 9]. Nevertheless, a probable explanation for the poor estimation of label uncertainty in valence is that the uncertainty layer, shared between arousal and valence, fits the $P(w|D)$ exclusively for the s in arousal, the easier task in SER. The layer models the average degree of uncertainty μ_s to be similar across the two dimensions, while they are not (seen in Section 4.1).

5.3. Label Uncertainty BNN for SER

This work is the first in literature to study BNNs for SER. The BBB technique, adopted by the proposed model, use simple gradient updates and produce stochastic outputs, making them promising candidates for end-to-end uncertainty modeling. More crucially, they open up possibilities for training the model on a distribution of annotations rather than a less informative standard deviation estimate.

While the proposed model have several advantages, they also come with certain shortcomings. Firstly, they are influenced by the initialization of $P(w)$ and $P(w|D)$, thereby requires heuristics-based initialization for optimal performances. Secondly, in the model we assumed that \mathcal{Y}_t follows a Gaussian distribution, and had only $a = 6$ annotations available to model the distribution. This might sometimes lead to unstable \mathcal{L}_{KL} during approximation of \mathcal{Y}_t , thereby affecting the training processes. Acknowledging that gaining more annotation is resource inefficient, as future work, we will investigate techniques to model stable \mathcal{Y}_t with limited annotations.

6. CONCLUSION

In this work, we introduced a BNN-based end-to-end approach for SER, which can account for the subjectivity and label uncertainty in emotional expressions. For this, we introduced a loss term based on the KL divergence to enable our approach to be trained on a distribution of annotations. Unlike previous approaches, our approach, with its stochastic outputs, can estimate both the mean and standard deviation of the emotion annotations. Analysis of the results reveal that the proposed uncertainty model trained on the KL loss term can aptly capture the distribution of emotion annotations in-terms of both the CCC and KL divergence, with a compromise on mean estimations. Moreover, we also showed that our approach, trained on raw audio signals, better captures label uncertainty in the arousal dimension of emotional expressions than the valence dimension.

7. REFERENCES

- [1] J. E. LeDoux and S. G. Hofmann, "The subjective experience of emotion: a fearful view," *Current Opinion in Behavioral Sciences*, vol. 19, pp. 67–72, 2018.
- [2] Z. Lei and N. Lehmann-Willenbrock, "Affect in meetings: An interpersonal construct in dynamic interaction processes," in *The Cambridge handbook of meeting science*. Cambridge University Press, 2015, pp. 456–482.
- [3] L. Nummenmaa, R. Hari, J. K. Hietanen, and E. Glerean, "Maps of subjective feelings," *Proceedings of the National Academy of Sciences*, vol. 115, no. 37, pp. 9198–9203, 2018.
- [4] B. W. Schuller, "Speech emotion recognition: two decades in a nutshell, benchmarks, and ongoing trends," *Communications of the ACM*, vol. 61, no. 5, pp. 90–99, Apr. 2018.
- [5] D. Dukes, K. Abrams, R. Adolphs, M. E. Ahmed, A. Beatty, K. C. Berridge, S. Broomhall, T. Brosch, J. J. Campos, Z. Clay et al., "The rise of affectivism," *Nature Human Behaviour*, pp. 1–5, 2021.
- [6] M. Abdelwahab and C. Busso, "Active learning for speech emotion recognition using deep neural network," in *2019 8th Int. Conf. on Affective Computing and Intelligent Interaction (ACII)*. IEEE, 2019.
- [7] J. Han, Z. Zhang, Z. Ren, and B. Schuller, "Exploring perception uncertainty for emotion recognition in dyadic conversation and music listening," *Cognitive Computation*, pp. 1–10, 2020.
- [8] P. Tzirakis, J. Zhang, and B. W. Schuller, "End-to-End Speech Emotion Recognition Using Deep Neural Networks," in *ICASSP - Int. Conf. on Acoustics, Speech and Signal Processing*, 2018, pp. 5089–5093.
- [9] P. Tzirakis, J. Chen, S. Zafeiriou, and B. Schuller, "End-to-end multimodal affect recognition in real-world environments," *Information Fusion*, vol. 68, pp. 46–53, 2021.
- [10] J. Han, Z. Zhang, M. Schmitt, M. Pantic, and B. Schuller, "From hard to soft: Towards more human-like emotion recognition by modelling the perception uncertainty," in *Proceedings of the 25th ACM Int. Conf. on Multimedia*, 2017, pp. 890–897.
- [11] K. Sridhar and C. Busso, "Modeling uncertainty in predicting emotional attributes from spontaneous speech," in *ICASSP - IEEE Int. Conf. on Acoustics, Speech and Signal Processing*, 2020, pp. 8384–8388.
- [12] H. Gunes and B. Schuller, "Categorical and dimensional affect analysis in continuous input: Current trends and future directions," *Image and Vision Computing*, vol. 31, no. 2, pp. 120–136, 2013.
- [13] R. Zheng, S. Zhang, L. Liu, Y. Luo, and M. Sun, "Uncertainty in bayesian deep label distribution learning," *Applied Soft Computing*, 2021.
- [14] S. Kohl, B. Romera-Paredes, C. Meyer, J. De Fauw, J. R. Ledsam, K. Maier-Hein, S. Eslami, D. Jimenez Rezende, and O. Ronneberger, "A probabilistic u-net for segmentation of ambiguous images," *Advances in Neural Information Processing Systems*, vol. 31, 2018.
- [15] M. Garnelo, D. Rosenbaum, C. Maddison, T. Ramalho, D. Saxton, M. Shanahan, Y. W. Teh, D. Rezende, and S. A. Eslami, "Conditional neural processes," in *Int. Conf. on Machine Learning*. PMLR, 2018, pp. 1704–1713.
- [16] C. Blundell, J. Cornebise, K. Kavukcuoglu, and D. Wierstra, "Weight uncertainty in neural network," in *International Conference on Machine Learning*. PMLR, 2015, pp. 1613–1622.
- [17] R. Reisenzein, "Pleasure-arousal theory and the intensity of emotions," *Journal of personality and social psychology*, vol. 67, no. 3, p. 525, 1994.
- [18] J. A. Russell, "A circumplex model of affect," *Journal of personality and social psychology*, vol. 39, no. 6, p. 1161, 1980.
- [19] M. K. T. E. Sanchez, G. Tzimiropoulos, T. Giesbrecht, and M. Valstar, "Stochastic Process Regression for Cross-Cultural Speech Emotion Recognition," in *Proc. Interspeech 2021*, 2021, pp. 3390–3394.
- [20] F. Ringeval, A. Sonderegger, J. Sauer, and D. Lalanne, "Introducing the RECOLA multimodal corpus of remote collaborative and affective interactions," in *10th IEEE Int. Conf. and Workshops on Automatic Face and Gesture Recognition (FG)*, 2013, pp. 1–8.
- [21] N. Raj Prabhu, C. Raman, and H. Hung, "Defining and Quantifying Conversation Quality in Spontaneous Interactions," in *Comp. Pub. of 2020 Int. Conf. on Multimodal Interaction*, 2020, pp. 196–205.
- [22] M. Valstar, J. Gratch, B. Schuller, F. Ringeval, D. Lalanne, M. Torres Torres, S. Scherer, G. Stratou, R. Cowie, and M. Pantic, "AVEC 2016: Depression, Mood, and Emotion Recognition Workshop and Challenge," in *Proceedings of the 6th International Workshop on Audio/Visual Emotion Challenge*, ser. AVEC '16. New York, NY, USA: Association for Computing Machinery, 2016, pp. 3–10. [Online]. Available: <https://doi.org/10.1145/2988257.2988258>
- [23] M. Grimm and K. Kroschel, "Evaluation of natural emotions using self assessment manikins," in *IEEE Workshop on Automatic Speech Recognition and Understanding*, 2005. IEEE, 2005, pp. 381–385.
- [24] G. Trigeorgis, F. Ringeval, R. Brueckner, E. Marchi, M. A. Nicolaou, B. Schuller, and S. Zafeiriou, "Adieu features? end-to-end speech emotion recognition using a deep convolutional recurrent network," in *2016 Int. Conf. on acoustics, speech and signal processing (ICASSP)*. IEEE, 2016.
- [25] I. Goodfellow, Y. Bengio, and A. Courville, *Deep Learning*, 3rd ed., ser. 5. The address of the publisher: MIT Press, 7 2016, vol. 4, ch. 3, pp. 51–77, <http://www.deeplearningbook.org>.
- [26] P. Tzirakis, A. Nguyen, S. Zafeiriou, and B. W. Schuller, "Speech emotion recognition using semantic information," in *ICASSP 2021-2021 IEEE International Conference on Acoustics, Speech and Signal Processing (ICASSP)*. IEEE, 2021, pp. 6279–6283.